



Aircraft evaluation of MODIS cloud drop number concentration retrievals

Scarlet R. Passer¹, Mikael K. Witte², and Patrick Y. Chuang¹

¹Earth and Planetary Sciences, University of California Santa Cruz, Santa Cruz, CA, USA

²Department of Meteorology, Naval Postgraduate School, Monterey, CA, USA

Correspondence: Patrick Y. Chuang (pchuang@ucsc.edu)

Received: 18 October 2024 – Discussion started: 28 November 2024

Revised: 2 April 2025 – Accepted: 3 April 2025 – Published: 13 August 2025

Abstract. Cloud drop number concentration (N_d) can be retrieved through passive satellite observation. These retrievals are useful due to their wide spatial and temporal coverage. However, the accuracy of the retrieved values is not well understood. In this study, we seek to understand why the retrievals agree or disagree with in situ measurements by examining the various cloud properties that underlie the retrievals. To do so, we compare satellite N_d derived from the Moderate Resolution Imaging Spectroradiometer (MODIS) instrument with in situ aircraft measurements made using a phase Doppler interferometer on board three flight campaigns sampling marine stratocumulus clouds. Intercomparison of N_d values shows that the discrepancy between retrieved and in situ N_d can be $\pm 50\%$ or more. In the mean, there is evidence of an overestimation bias by MODIS retrievals, although the sample size is insufficient for statistical certainty. We find that MODIS N_d is best interpreted as representative of the mid-cloud region, as there is almost always a greater discrepancy from in situ values near the cloud top and cloud base. We also find evidence of cases where N_d is accurately retrieved but the effective radius is not, presumably due to offsetting errors in other retrieval parameters. Vertical profiles of the extinction coefficient β , liquid water content L , and effective radius r_e measured during sawtooth-pattern flight legs through the cloud top are also compared to implicit MODIS retrieval profiles. For the two cases with N_d agreement, all profiles match well. For the six cases with significant disagreement, there is no consistent underlying cause. The discrepancy originates from one of the following: (a) discrepancy in the r_e profile, (b) discrepancy in the β and L profiles, or (c) discrepancy in both.

1 Introduction

Cloud drop number concentration (N_d) is a fundamental property of clouds. This property is relevant to numerous effects that clouds have on weather and climate. For example, clouds with higher N_d will have a larger albedo (assuming all else equal), which in turn will lead to a larger solar reflectance (Twomey, 1977). The ability of a warm (i.e., ice-free) cloud to form precipitation is also dependent on N_d . A cloud with very high N_d will not produce appreciable rainfall rates because the drops are unable to grow to the required sizes to efficiently sediment, while at the other extreme of very low N_d , warm clouds produce precipitation very effectively (Sorooshian et al., 2009). Understanding and evaluating aerosol–cloud interactions frequently involves N_d , as activation of particulate matter is one of the strongest connections between aerosol and clouds (Bellouin et al., 2020; Quaas et al., 2020; Gordon et al., 2023).

Passive satellite observation is one of the primary methods that we have to measure and understand the climatology of N_d at large spatial and temporal scales (e.g., Bennartz, 2007; McCoy et al., 2018, 2020; Christensen et al., 2022). The Moderate Resolution Imaging Spectroradiometer (MODIS) instrument on board the Terra and Aqua satellites is one important source of satellite observations of N_d . A review paper by Grosvenor et al. (2018) comprehensively surveys our understanding of N_d derived from remote sensing, so we focus this Introduction only on aspects that are directly relevant for this study. A theoretical analysis by Bennartz (2007) suggests that, for cloud fractions over 80 % and a liquid water path (LWP) $> 30 \text{ g m}^{-2}$, i.e., conditions relevant to the stratocumulus (Sc) clouds observed in this study, MODIS N_d re-

trievals should exhibit relative errors $< 80\%$, a value which Grosvenor et al. (2018) is in agreement with. These errors are mainly due to uncertainties in retrieving the effective radius r_e , LWP, cloud optical depth τ_c , and cloud fraction.

There are a handful of past studies that assess the agreement between in situ aircraft measurements and satellite retrievals of N_d . Painemal and Zuidema (2011) use data from the National Center for Atmospheric Research (NCAR) C-130 aircraft measuring Sc in the Southeast Pacific during the Variability of the American Monsoon Systems Ocean-Cloud-Atmosphere-Land Study (VOCALS). They find good agreement in the mean for the 19 cases that they examined, with the assumption that the liquid water profile is adiabatic. Of the 19 cases, two had large discrepancies (30 % to 50 % discrepancy) that they attribute to sub-adiabaticity. Their cases span a wide range, from $< 50 \text{ cm}^{-3}$ to $> 300 \text{ cm}^{-3}$. They also find that the assumption that N_d is constant with height is valid for their cases. However, Grosvenor et al. (2018) point out that their strong agreement occurs not necessarily because the underlying measurements are accurate but is due to an overestimate of the effective radius almost exactly offsetting an overestimate of the cloud adiabaticity. Min et al. (2012) also analyze data from VOCALS but combine NCAR C-130 and U.S. Department of Energy (DOE) G-1 aircraft data and find that, without accounting for adiabaticity, MODIS overestimates N_d relative to aircraft measurements, with a mean bias of 25 %. If measured adiabaticity is used, then no statistically significant bias is detected, with most of their 17 cases appearing to agree to within 50 % (two outliers are noted). A third study (Bennartz and Rausch, 2017) compares results from their updated algorithm to the same VOCALS results from Painemal and Zuidema (2011). They find a modest bias (less than 20 cm^{-3}) between aircraft and MODIS and an average uncertainty of $\sim 35 \text{ cm}^{-3}$. McCoy et al. (2018) utilize a much larger data set, but in order to do so, they greatly relax the requirements for the co-location of aircraft and satellite observations in both space and time. They compare aircraft measurements with the satellite retrieval averaged over 3 d for the closest $3^\circ \times 3^\circ$ area. They find the average agreement to be much poorer than that of these previous studies ($r^2 = 0.46$), but this may simply be a matter of not measuring the same cloud at the same time.

Gryspeerdt et al. (2022) compare many aircraft field campaigns with satellite-retrieved N_d , although only a subset of these focused on stratiform clouds. Their data set is a mixture of different instruments and different aircraft platforms. If we examine only their results from Sc projects, they find r^2 values between 0.5 and 0.75. Restricting the data using different filters can somewhat increase r^2 , though the range for Sc-only campaigns remains about the same. The best-fit slope of the in situ vs. MODIS data for Sc-only campaigns is, with one exception (discussed next), close to 1, suggesting no mean bias. Variability of the data is high, however, with many measurements disagreeing by a factor of 2 or more. The one project that is the exception, i.e., the project that exhibits sig-

nificant bias between in situ and satellite-derived N_d , is, surprisingly, from the analysis of NCAR C-130 data from VOCALS. The slope is very noticeably different from 1, with MODIS exhibiting larger values relative to the aircraft. This result appears to disagree with the three other studies that focus on VOCALS (described above). The source of this disagreement is unclear.

Broadly speaking, these comparisons, with some exceptions, paint a rather optimistic picture for N_d retrievals. Most of these studies suggest that MODIS retrievals are better than the theoretical 80 % relative uncertainty proposed by Bennartz (2007), albeit these are not all the same retrievals (many of the studies filter the data in various ways to assess which conditions are most favorable for an accurate retrieval). However, given that many of these studies focus on the VOCALS field campaign and utilize in situ cloud probes with the same operating principle (with Gryspeerdt et al., 2022, being the exception to both), it would be informative to broaden the type of cloud and instrument used for evaluating satellite N_d retrievals. There are reasons to believe that the in situ measurements on board the C-130 from the VOCALS campaign may have biases. Past studies (e.g. Painemal and Zuidema, 2011) attribute biases between the in situ and MODIS-retrieved effective radius from VOCALS to issues with the satellite retrievals (e.g., due to three-dimensional radiative effects or unresolved horizontal heterogeneity). However, Witte et al. (2018), using aircraft data from a phase Doppler interferometer (PDI) during three different Sc field campaigns, find no bias between in situ and MODIS r_e . They instead find that the bias when using the older cloud probes is correlated with the breadth of the drop size distribution, which they attribute to difficulties that such probes have measuring larger drops. However, this issue may affect the estimation of r_e differently than for N_d , so it is unclear what the consequences are, if any, of such instrument limitations.

The focus of this study is to compare MODIS retrievals against in situ measurements from three Sc-focused field campaigns using PDI data from the Twin Otter in order to evaluate the accuracy of the satellite N_d product. These are the same data sets as used in Witte et al. (2018). Importantly, we also evaluate the validity of the assumptions underlying the retrievals through an analysis of the vertical profiles of cloud properties, which, to our knowledge, previous studies have not examined in detail. When we find good agreement, is it because the underlying properties are also in agreement, or are there cases of canceling errors? When we find poor agreement, is there one consistent reason for it, or is there a diversity of reasons?

1.1 Satellite N_d retrieval

The most common method for retrieving the number concentration utilizes the following equation (Grosvenor et al.,

2018):

$$N_d = \frac{\sqrt{5}}{2\pi k} \left(\frac{f_{ad} c_w \tau_c}{Q_{ext} \rho_w r_e^5} \right)^{1/2}. \quad (1)$$

Cloud optical depth τ_c and cloud top effective radius r_e are the two (mostly) independently retrieved quantities used in the N_d retrieval, where r_e is defined as

$$r_e = \frac{\int_0^\infty r^3 n(r) dr}{\int_0^\infty r^2 n(r) dr}, \quad (2)$$

where $n(r)$ is the drop size distribution as a function of the drop radius r . Retrieved N_d is more sensitive to the same relative uncertainty in retrieved r_e than τ_c due to the difference in the magnitude of the exponents (5/2 versus 1/2) in Eq. (1). Density of water ρ_w is known, and the remaining variables (adiabatic fraction f_{ad} , water content lapse rate c_w , a constant that relates the mean-volume and effective radii k , and the extinction efficiency factor Q_{ext}) are considered fixed as described below. To produce an estimate of r_e from aircraft suitable for comparison with that from MODIS, a weighting function is used to weight the impact of the cloud vertical structure on the aircraft-derived variables (Platnick, 2000):

$$W(\tau_c) = a \tau_c^b \exp \left(-\tau_c \left(\frac{1}{\mu} + \frac{1}{\mu_0} \right) \right). \quad (3)$$

Here, $b = 2$, a is a normalization constant, and μ and μ_0 are the cosine of the sensor and solar zenith angles, respectively. The weighting function describes, as a function of the cloud optical depth, how much influence the measurement from a given region of a cloud has on satellite-derived variables. This function peaks within a few tens of meters of cloud top (Platnick, 2000; Witte et al., 2018), and therefore the effective radius reflects values in this cloud top region.

Cloud optical depth τ_c is defined as the vertical integral of the extinction coefficient $\beta(z)$:

$$\tau_c = \int_{z_{base}}^{z_{top}} \beta(z) dz, \quad (4)$$

where z_{top} and z_{base} are the altitude of the cloud top and cloud base, respectively.

At any altitude, $\beta(z)$ is related to the cloud drop size distribution $n(r, z)$, for which we now include the dependence on altitude z :

$$\beta(z) = \int_0^\infty \pi Q_{ext} n(r, z) r^2 dr. \quad (5)$$

The remaining variables in the N_d retrieval (Eq. 1) are described as follows.

1. N_d is assumed to be a constant with respect to height in the cloud; i.e., $N_d(z) = \text{constant}$.

2. k is defined as

$$k = \left(\frac{r_v}{r_e} \right)^3, \quad (6)$$

where r_v is the volume-mean drop radius. The MODIS retrieval assumes that $k = 0.8$. Previous studies suggest that k is well-constrained in stratocumulus clouds, typically ranging between 0.7 and 0.9 (Miles et al., 2000; Lebsock and Witte, 2023).

3. Q_{ext} is the extinction efficiency (dimensionless) and represents the ratio between the extinction and geometric cross sections of a drop. It is a function of the drop radius r , but because the radius of the drops of interest is usually much larger than the wavelengths of light used for the retrievals, it can be assumed that $Q_{ext} = 2$ (the limit for geometric optics) (Platnick, 2000).
4. c_w is the adiabatic gradient of liquid water content L with respect to height and is a weak function of temperature and pressure. From Eq. (14) in Grosvenor et al. (2018), we compute a value of $c_w = 2.3 \times 10^{-6} \text{ kg m}^{-4}$. We assume c_w to be constant vertically through a cloud, which should introduce an error that is less than 1 % because the stratocumulus clouds observed in this study are quite geometrically thin ($< 500 \text{ m}$) (Grosvenor et al., 2018).
5. f_{ad} is defined as the fraction of cloud liquid water content relative to its adiabatic value at a given height above the cloud base. The MODIS retrieval assumes $f_{ad} = 0.6$. Combining the definitions of c_w and f_{ad} yields the profile of liquid water content:

$$L(z) = f_{ad} c_w (z - z_{base}). \quad (7)$$

Implicit retrieval profiles

The MODIS retrieval implicitly assumes specific vertical profiles of r_e , β , and L . These profiles, along with the cloud base height, can be derived as follows.

1. The cloud top liquid water content is computed as

$$L(z_{top}) = \frac{4}{3} \pi \rho_w \cdot k r_e^3(z_{top}) \cdot N_d. \quad (8)$$

2. The liquid water content profile $L(z)$ is defined above (Eq. 7).
3. Cloud base height z_{base} is determined by the altitude where $L(z) = 0$. By re-arranging Eq. (7) and applying it at $z = z_{top}$, we get

$$z_{base} = z_{top} - L(z_{top}) / f_{ad} c_w. \quad (9)$$

4. $r_e(z)$ is derived starting from the definition of r_v :

$$\frac{4}{3}\pi r_v^3(z) N_d \rho_w = \frac{4}{3}\pi \left[k r_e^3(z) \right] N_d \rho_w = L(z).$$

This can be re-arranged in terms of r_e :

$$r_e(z) = \left[\frac{3}{4\pi \rho_w k} \frac{L(z)}{N_d} \right]^{1/3}. \quad (10)$$

5. $\beta(z)$ is derived by substituting the definitions of r_e and L into Eq. (5), which yields (Grosvenor et al., 2018)

$$\beta(z) = \frac{3}{4} \frac{Q_{\text{ext}}}{\rho_w} \frac{L(z)}{r_e(z)}. \quad (11)$$

In order to better identify the source of any discrepancies between MODIS and in situ N_d , the vertical profiles $r_e(z)$, $\beta(z)$, and $L(z)$ that are inherent in the MODIS algorithm for estimating N_d will be compared to in situ observations of the same quantities, along with cloud base height z_{base} . There are a number of potential sources of uncertainty, including the MODIS retrievals of r_e and τ_c , as well as the validity of the above assumptions.

2 Methods

2.1 In situ observations of N_d

2.1.1 Aircraft observations

In situ data were acquired during three different flight campaigns that sampled marine stratocumulus clouds: the Marine Stratus/Stratocumulus Experiment (MASE; Lu et al., 2007), the Physics of Stratocumulus Top experiment (POST; Carman et al., 2012; Gerber et al., 2013), and VOCALS (Mecho et al., 2014; Zheng et al., 2011). All three of these campaigns used a phase Doppler interferometer (PDI) on board the CIRPAS Twin Otter (TO) aircraft to derive cloud microphysical properties. See Chuang et al. (2008) for details about the PDI measurement method and data processing.

The MASE campaign was flown in the Northeast Pacific near Monterey, California, during July 2005. VOCALS was centered off the coast of Chile in the Southeast Pacific and was flown from October to November of 2008. Flights during the MASE and VOCALS campaigns utilized level legs (i.e., flight segments flown at constant altitude and heading for a sustained period, usually 10 min for the flights analyzed in this work), which sampled from below the cloud base to near the cloud top. POST was flown slightly farther offshore in a similar location as for MASE, during July and August of 2008. From the POST campaign, we analyze flight legs that were flown in a sawtooth pattern, flying repeatedly up and down between ~ 100 m below the cloud top to ~ 100 m above. Overall, we analyze four flight days from MASE, 10 from VOCALS, and eight from the POST campaign, as these

flights coincide with a MODIS overpass. More details on matching the aircraft flights with MODIS overpasses can be found in Witte et al. (2018).

The PDI measurements from these three field campaigns have been used to analyze the retrieval of the cloud effective radius from MODIS. Previous studies (Painemal and Zuidema, 2011; Min et al., 2012; Noble and Hudson, 2015) have suggested that MODIS retrievals of r_e are biased high by 2 to 5 μm relative to in situ measurements, but using the same data set as in this study, Witte et al. (2018) found no such bias, with MODIS and in situ measurements agreeing within 0.7 μm in the mean. They attribute observed bias to issues with the in situ aircraft instrumentation used in previous studies. This consideration suggests that, in the mean, there is no bias in retrievals of N_d due to a bias in retrieved r_e , an assertion that we will evaluate as part of our analysis.

2.1.2 In situ N_d and r_e calculations

To estimate the cloud drop number concentration from PDI, in-cloud sampling legs are analyzed for each flight. To be consistent with MODIS, data from near the cloud top are used to derive r_e . In contrast, because the satellite retrieval assumes N_d is constant throughout the cloud, mid-cloud data are used to derive the number concentration, as this location is more representative of the mean cloud N_d value relative to the cloud top values (as will be shown below).

For the VOCALS and MASE campaigns, we analyze the mid-cloud and cloud top level legs. However, the POST campaign primarily used a sawtooth flight pattern. Therefore, we define cloud top as the altitude where liquid water content crosses a threshold of $L = 0.05 \text{ g m}^{-3}$, a commonly used threshold in the airborne science community. The effective radius is calculated from within 10 m of this cloud top. We use the range between 60 to 90 m below the cloud top as an analog to level mid-cloud legs to calculate a representative value of N_d during POST. While this altitude range does not correspond to “mid-cloud” in the sense of cloud geometric thickness, this region is typically far enough from the cloud top to avoid the impacts of entrainment mixing.

For ease in comparing MODIS implicit cloud profile estimations to observation, we create a shifted altitude (z_{shift}) for POST, which is defined by $z_{\text{shift}} = 0$ at the cloud top; i.e., $z_{\text{shift}} = z - z_{\text{top}}$. To perform this coordinate transformation, we determine the altitude of the cloud top (z_{top}) for each individual ascent or descent (or “leg”) of the sawtooth flight path (using the threshold $L = 0.05 \text{ g m}^{-3}$). All in situ measurements for each leg are referenced to z_{shift} for that leg. More details about the altitude shifting process can be found in Carman et al. (2012).

For the purpose of making a more like-to-like comparison between PDI and MODIS, the number concentration and effective radius measured along their respective legs are averaged over 1 km (20 s) intervals to match the MODIS spatial resolution. The mean and variability of N_d and r_e for each

10 min (or ≈ 30 km at a mean true airspeed of 55 m s^{-1}) flight leg are calculated from these 1 km average values, which is the uncertainty that we show in the results (below). This variability does not reflect any uncertainty due to differences in the spatial domain sampled, as well as any temporal differences in the sampling, which are difficult to assess.

The main source of instrumental uncertainty is the uncertainty in the instrument view volume. The view volume, in units of volume of air sampled per second, is the product of three values. The first is the probe “length”, which is calculated for each flight from the collected data itself (using the method from Chuang et al., 2008), so day-to-day variation should be accounted for to well within 5 %. The second value is the aircraft true air speed, which is known quite accurately, almost certainly to within 5 %. The third value is the probe “width”, which is fixed by the optical hardware. Recent in-depth laboratory examination of this subject (Landro, 2023) suggests that this width may be smaller than the theoretical value for very small drops, which would lead to an under-estimation of N_d , but mostly affects larger values of N_d (which tend to exhibit smaller drop sizes). We estimate that this bias could be as large as 10 % for $N_d > 400 \text{ cm}^{-3}$ and decreases to less than 1 % for $N_d < 100 \text{ cm}^{-3}$. Counting uncertainty is unlikely to be significant because many thousands of drops are observed for any given data point, so the Poisson standard deviation of \sqrt{n} would suggest an uncertainty of < 1 %. These instrumental uncertainties, when combined, produce an uncertainty of less than 20 %, which is almost always smaller than the observed spatiotemporal variability, which is why we report the latter.

2.1.3 Profile calculations

The N_d retrieval combines measurements of τ_c and cloud top r_e with assumptions about the cloud vertical structure (see Sect. 1.1). Therefore, specific vertical profiles of the effective radius, liquid water content, and extinction coefficient are implicitly assumed. Due to the sawtooth sampling strategy during the POST campaign, we can compare these assumed profiles with observations. We also evaluate the assumptions that k and f_{ad} are constant.

The profiles of L , r_e , and β are derived directly from cloud drop size distributions measured by the PDI and binned over 5 m increments within z_{shift} space. Consistent with the satellite retrieval (Eq. 1), we also assume $Q_{\text{ext}} = 2$ when calculating β . To determine the adiabatic liquid water content $L_{ad}(z)$, first, the mean altitude for the near-cloud base is identified using a threshold liquid water content of $L = 0.1 \text{ g m}^{-3}$. Next, c_w is used to extrapolate downward to $L = 0 \text{ g m}^{-3}$, associated with the true cloud base z_{base} .

2.2 Satellite retrieval details and sampling methodology

We utilize MODIS collection 6.1 level 2 retrievals of r_e and τ_c using the $2.1 \mu\text{m}$ band (“Cloud_Effective_Radius” and “Cloud_Optical_Thickness” products, respectively) from both Aqua and Terra, consistent with the approach of Witte et al. (2018). Over the small sample size considered here, we find no evidence of systematic differences between satellites. Number concentration N_d is then calculated from r_e and τ_c using Eq. (1). A full description of the MODIS sampling methodology is given in Witte et al. (2018). Briefly, we analyze flight legs that occurred within 90 min of MODIS overpasses that covered the flight sampling area (most retrievals were within 30 min of their associated aircraft leg). We then select a 25 km^2 ($5 \text{ pixels} \times 5 \text{ pixels}$) area centered on the mean coordinates of the aircraft leg to compare with in situ measurements.

2.3 Uncertainty calculations

The uncertainty of any variable x is expressed as the 95 % margin of error:

$$\text{error} = \frac{\sigma_x}{\sqrt{n_x}} z(0.95), \quad (12)$$

where σ_x is the standard deviation of x , n_x represents the total number of measurements, and the quantity $z(0.95)$ is the z score for the 95 % confidence interval and has a value of 1.96. We choose margin of error versus standard error to reflect uncertainty in unsampled spatial variability because the aircraft samples a narrow transect through a $1 \text{ km} \times 1 \text{ km}$ box, while MODIS senses photons arriving from the entire area.

The MODIS uncertainty is calculated from 1 km measurements over a 25 km^2 area. PDI uncertainty is calculated from downsampled 1 km measurements over the relevant time interval of a given flight leg. Both the MODIS and PDI uncertainties are a reflection of spatial variability at 1 km. This measurement does not reflect instrumental uncertainty or error in the assumptions.

3 Results

We first analyze N_d and r_e for all three campaigns. After that, we capitalize on the sawtooth legs from the POST flights to compare the profiles of k , f_{ad} , r_e , β , and L .

3.1 Comparison between MODIS and PDI N_d

Figure 1 compares MODIS and PDI N_d for all three flight campaigns. Though the majority of flights agree to within 50 % (accounting for variability), there are several cases that exceed this range. Of those cases, most are overestimates by MODIS, with the one exception being VOCALS

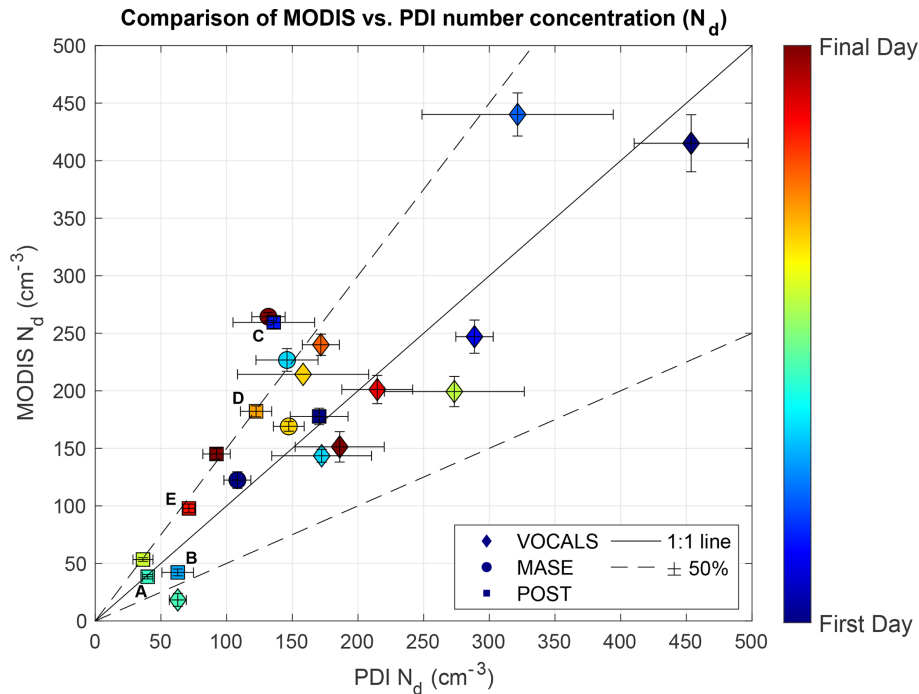


Figure 1. Comparison of MODIS number concentration vs. PDI number concentration. PDI values are N_d averaged at mid-cloud for all flight legs on that day, and the uncertainty bar represents the 1σ variability of 1 km averaged values. Each flight campaign is marked by a symbol with a color ranging from the first day of the campaign to the last. Several POST days are labeled A to E, which represent specific cases discussed in Sect. 3.3. The MODIS N_d value is a 1 km average of a $5\text{ km} \times 5\text{ km}$ swath (with 1σ variability uncertainty bars) obtained using Eq. (1), where the effective radius and optical depth are taken from the satellite products. A linear fit of the data produces a slope of 1.1 ± 0.14 .

day 1 November 2008 (teal diamond in Fig. 1). At a population level, linear regression yields a slope of 1.1 ± 0.14 (95 % confidence interval). Although the one-to-one line is included in this confidence interval, there is a suggestion of an overestimation bias. However, because of the limited sample size, it is unclear if this is statistically significant.

There are several questions that arise from this result. First, when the MODIS and PDI number concentration are in very good agreement (i.e., within sampling uncertainty of each other), is the satellite-retrieved N_d correct for the right underlying reasons, or are there multiple errors that offset each other? Second, when MODIS disagrees with PDI, which MODIS retrieval products and/or assumptions are responsible for the discrepancy? To investigate these questions, we further analyze and compare the underlying variables in the MODIS N_d retrieval.

3.2 Comparison between MODIS and PDI $r_e^{5/2}$

Effective radius is the most influential term in the N_d calculation, and thus it is logical to speculate that good agreement between satellite and in situ r_e values would manifest as good agreement between the PDI and MODIS number concentration. Because $\text{MODIS } N_d \propto r_e^{-5/2}$ (Eq. 1), Fig. 2 compares MODIS and in situ $r_e^{5/2}$ values across the three campaigns.

Figure 2 shows that there is a range of agreement between PDI and MODIS, with most of the days agreeing to within 25 %. A linear regression of the data produces a slope of 1.0 ± 0.07 (95 % confidence interval). This result is consistent with Witte et al. (2018), who found no significant bias between MODIS- and PDI-measured r_e . Additionally, if r_e was the determining factor in the accuracy of MODIS N_d retrievals, it would be expected that the potential high bias of MODIS N_d (Fig. 1) would correspond to a low bias in MODIS r_e . The data do not support this hypothesis, implying that the problem with the satellite estimation cannot solely be attributed to the effective radius.

On an individual flight basis, comparing Fig. 2 and Fig. 1 shows that agreement in N_d does not necessarily equate to agreement in $r_e^{5/2}$ and vice versa. In fact, there are four different scenarios that occur:

1. agreement in $r_e^{5/2}$ with agreement in N_d ,
2. agreement in $r_e^{5/2}$ with disagreement in N_d ,
3. disagreement in $r_e^{5/2}$ with agreement in N_d ,
4. disagreement in $r_e^{5/2}$ with disagreement in N_d .

We illustrate one example of each case in Table 1. The finding that the r_e retrieval does not govern agreement of MODIS

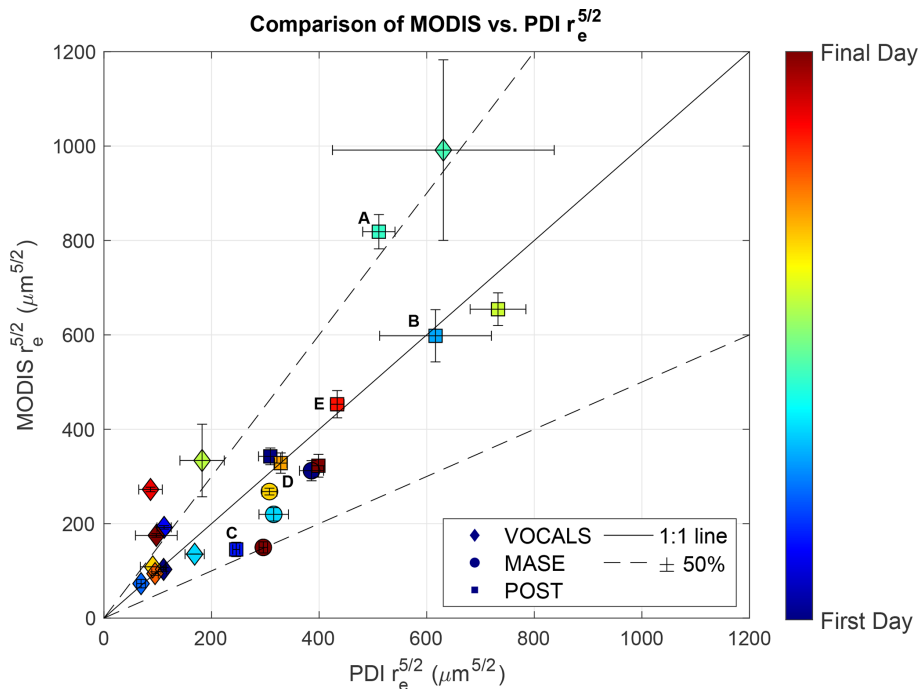


Figure 2. Comparison of $r_e^{5/2}$ between PDI measurements and the MODIS-retrieved values. Satellite effective radius is the average of $5\text{ km} \times 5\text{ km}$ swaths of the MODIS r_e product. The PDI value is r_e averaged for all cloud top flight legs on that day. A linear fit of the data produces a slope of 1.0 ± 0.07 . Labels and uncertainty bars are the same as in Fig. 1.

Table 1. Examples of each of the four possible combinations of N_d and r_e agreement with their associated campaign, day, discrepancy, and corresponding symbol from Figs. 1 and 2. The finding that at least one case has a large discrepancy (37 %) in effective radius with a small discrepancy (4 %) in N_d implies that there are compensating errors in other retrieval parameters. In other words, it is possible to retrieve the right N_d for the wrong underlying reasons.

Good N_d agreement					
	Symbol	Campaign	Date	% discrepancy r_e	% discrepancy N_d
Good r_e agreement	■	POST	16 July 2008	−6.8	+4.1
Poor r_e agreement	◆	VOCALS	10 November 2008	+37.0	+4.0
Poor N_d agreement					
	Symbol	Campaign	Date	% discrepancy r_e	% discrepancy N_d
Good r_e agreement	■	POST	4 August 2008	−0.04	+33
Poor r_e agreement	◆	VOCALS	1 November 2008	+17	−250

N_d leads us to further investigate the other variables in the MODIS N_d calculation.

3.3 Specific POST cases

The MODIS calculation for the number concentration implicitly relies on the vertical profiles of L , r_e , and β . These profiles combine MODIS measurements of τ_c and r_e with assumptions of cloud vertical structure (see Sect. 1.1). We compare these profiles with those measured by aircraft during the POST campaign. The sawtooth flight plan of POST

allows for detailed profile comparisons. Five POST cases are selected to illustrate the range of behaviors observed across all eight POST flights analyzed in this manner. Figure 3 illustrates the amount of data for four of the cases. Most of the data is concentrated within 150 m of the cloud top. It is difficult to make statistically robust conclusions at altitudes below this region. Within these eight cases, we find two with excellent agreement between all observed and retrieved properties (one of which is explored in depth; see Case A). The other six are cases where N_d is not accurately retrieved. Among these cases, none represents an accurate retrieval of

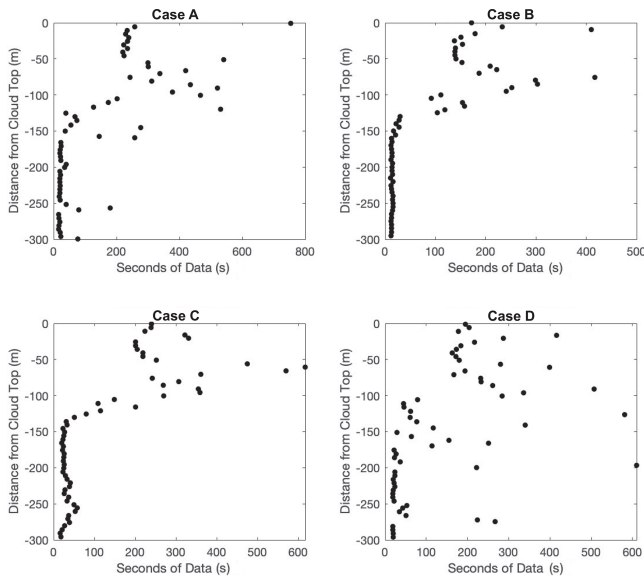


Figure 3. Amount of data for four of the five POST flights selected for additional analysis. Points represent seconds of non-zero data within each 5 m z_{shift} altitude bin and are concentrated within ~ 150 m of the cloud top.

N_d with significant errors in the underlying retrieval properties that compensate for each other, although such cases do exist (see Table 1).

3.3.1 Case A: POST day 30 July 2008

Case A (Fig. 4) is an example of the best-case scenario for agreement between MODIS and in situ profiles. The PDI observed number concentration (open circles) calculated at mid-cloud is $N_d = 40 \pm 2 \text{ cm}^{-3}$, while MODIS estimates $N_d = 38 \pm 4 \text{ cm}^{-3}$ (solid red line). The satellite assumes that this number concentration is fixed throughout the vertical cloud profile. In reality, N_d is not constant with height but instead gradually drops off towards the cloud base and cloud top. We attribute lower values of N_d near the cloud top to cloud drop evaporation due to turbulent entrainment of warm, dry air from above the boundary layer. Low values near the cloud base may be an effect of an uneven cloud base, which affects the altitude range over which activation causes N_d to increase with height. In addition, the cloud base is typically higher in those portions of the cloud layer that experience downdrafts due to lower adiabaticity (Zhou and Bretherton, 2019), which can affect N_d in the cloud base region. Through the middle of the cloud, N_d does appear reasonably constant on average. Because constant N_d is consistent with the MODIS assumption, we use this as justification for the use of mid-cloud level legs for the MODIS–PDI N_d comparison.

The vertical profiles of L , r_e , and β all agree very closely during this flight. The MODIS estimate of the cloud top r_e (blue star) is plotted at an altitude determined by the weight-

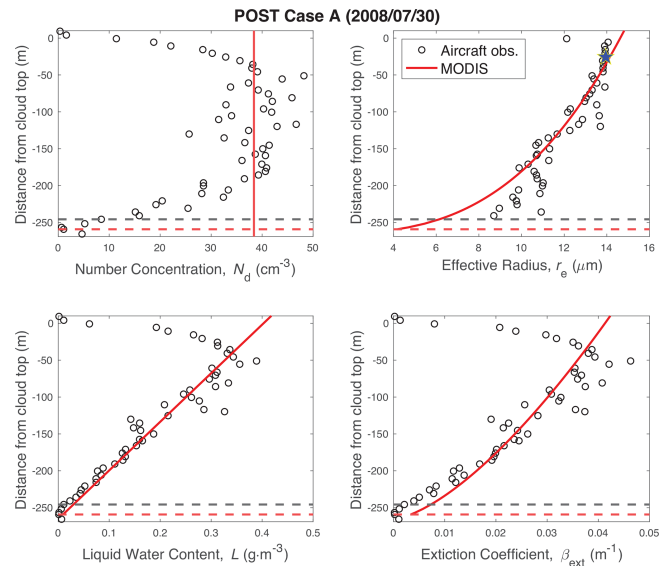


Figure 4. Profiles of N_d , r_e , L , and β for POST Case A (30 July 2008) comparing aircraft data (circles) and MODIS retrieval profiles (red lines). The aircraft-measured cloud base is the black dashed line, while the MODIS-estimated cloud base is the red dashed line. Aircraft-derived r_e that most closely corresponds to the MODIS cloud top value is indicated by the blue star and is placed at an altitude determined by the max weight from Eq. (3). The MODIS retrieval profiles of N_d , r_e , L , and β are based on Eqs. (1), (10), (7), and (11), respectively.

ing function (Eq. 3) and is consistent with the aircraft measurements. Lastly, the cloud base altitudes estimated by MODIS and the aircraft (red and black dashed lines, respectively) also agree well. The alignment between this full set of MODIS and aircraft observations results in an accurate estimate of N_d as long as we interpret this value as a mid-cloud estimate. However, this day represents only two of the flights where agreement across all quantities occurs.

3.3.2 Case B: POST day 21 July 2008

Unlike the strong agreement between MODIS and PDI seen in Case A, Case B (Fig. 5) illustrates a day in which all of the profiles have very poor agreement. The MODIS-retrieved number concentration is $N_d = 42 \pm 12 \text{ cm}^{-3}$, while the in situ value is $N_d = 63 \pm 3 \text{ cm}^{-3}$. This disagreement occurs despite the fact that the satellite cloud top effective radius (blue star) is well-matched to the PDI estimate ($13.0 \pm 0.9 \mu\text{m}$ vs. $13.0 \pm 0.5 \mu\text{m}$), indicating that cloud top r_e is not the source of the N_d disagreement.

While the MODIS and PDI r_e profiles agree at the cloud top, at all other altitudes, MODIS greatly underestimates the effective radius. All else being equal, this should lead to an overestimation of N_d , which is not what we see. Instead, we attribute the MODIS N_d underestimation to disagreement with the MODIS τ_c retrieval. Any error in MODIS τ_c propa-

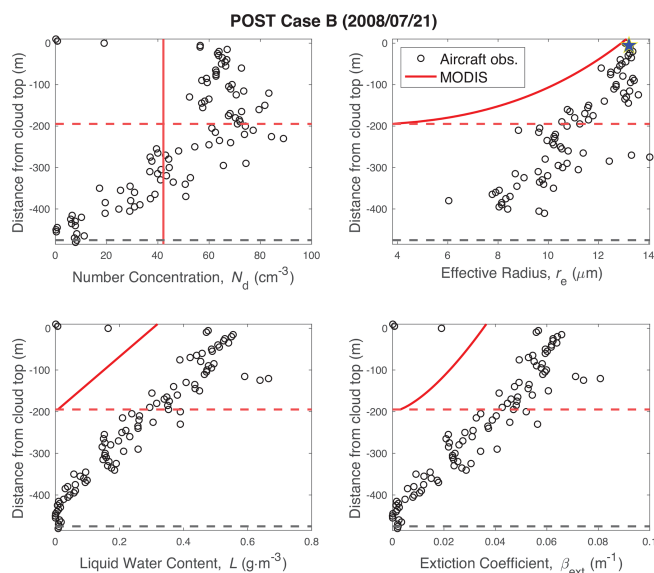


Figure 5. Comparison of profiles of N_d , r_e , L , and β from aircraft observations (circles) and MODIS retrievals (red lines) for POST Case B (21 July 2008). See Fig. 4 for more details.

gates to both the β and L profiles. Integration of the MODIS β profile results in a τ_c value smaller than observed, leading to an underestimation of N_d ($N_d \propto \tau_c^{1/2}$), as seen in Fig. 5, as well as a cloud base that is too high, which is equivalent to a cloud that is too thin.

3.3.3 Case C: POST day 17 July 2008

During POST flight 2008/17/07, the MODIS number concentration is $N_d = 260 \pm 31 \text{ cm}^{-3}$, almost twice the PDI value of $N_d = 140 \pm 5 \text{ cm}^{-3}$ (Fig. 6). In contrast to Case B, we attribute the cause of this disagreement to the MODIS-retrieved cloud top r_e . The β and L profiles are in close agreement, presumably because the MODIS- and PDI-derived τ_c are in agreement. However, both the PDI cloud top r_e and the PDI r_e vertical profile are greater than the MODIS estimates, leading to the large overestimation of N_d .

3.3.4 Case D: POST day 4 August 2008

MODIS overestimates the number concentration during POST Case D (4 August 2008), finding an $N_d = 180 \pm 12 \text{ cm}^{-3}$ compared to a PDI value of $N_d = 122 \pm 5 \text{ cm}^{-3}$ (Fig. 7). This case illustrates a day when the assumption that N_d is constant with altitude is not accurate, with the retrieval overestimating N_d at all altitudes. The r_e subplot shows that there is good agreement between PDI and MODIS in both the cloud top r_e value and the r_e vertical profile (in the region of most influence, i.e., within 50 m of the cloud top). However, the MODIS β and L profiles differ to a substantial degree from the PDI profiles. The MODIS β profile is greater than what is

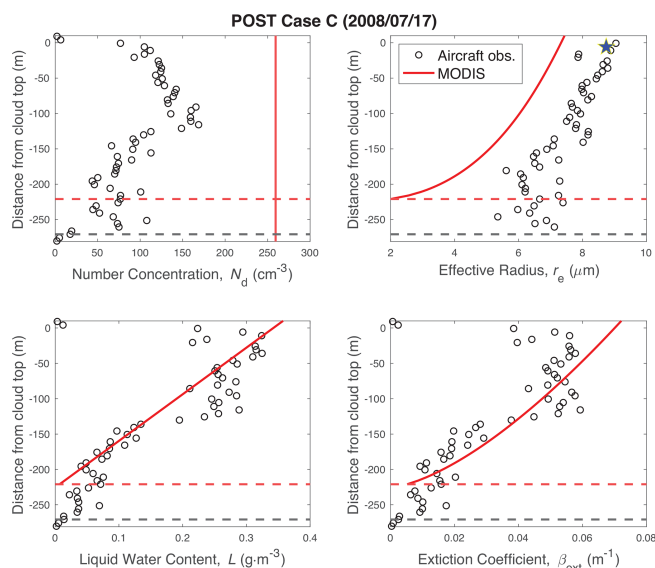


Figure 6. Comparison of profiles of N_d , r_e , L , and β from aircraft observations (circles) and MODIS retrievals (red lines) for POST Case C (17 July 2008). See Fig. 4 for more details.

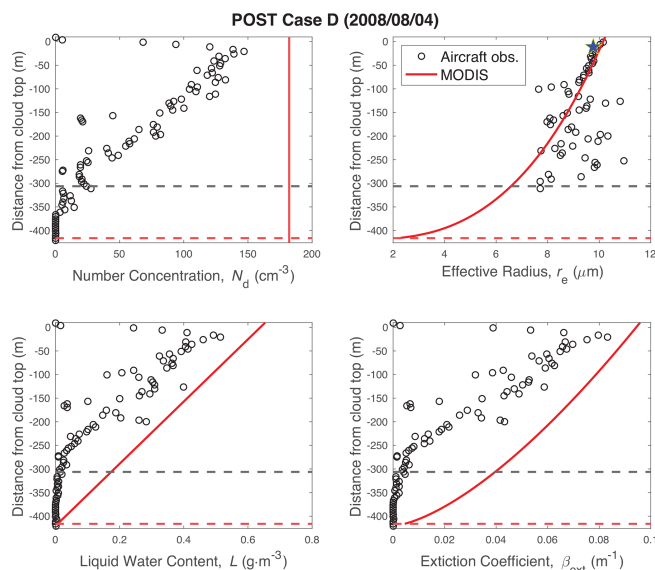


Figure 7. Comparison of profiles of N_d , r_e , L , and β from aircraft observations (circles) and MODIS retrievals (red lines) for POST Case D (4 August 2008). See Fig. 4 for more details.

observed, meaning that the MODIS τ_c is also greater than the PDI value. Due to the relationship between τ_c and N_d , it follows that an overestimation of MODIS optical depth should lead to an overestimation of N_d , which is indeed what we see in Fig. 7.

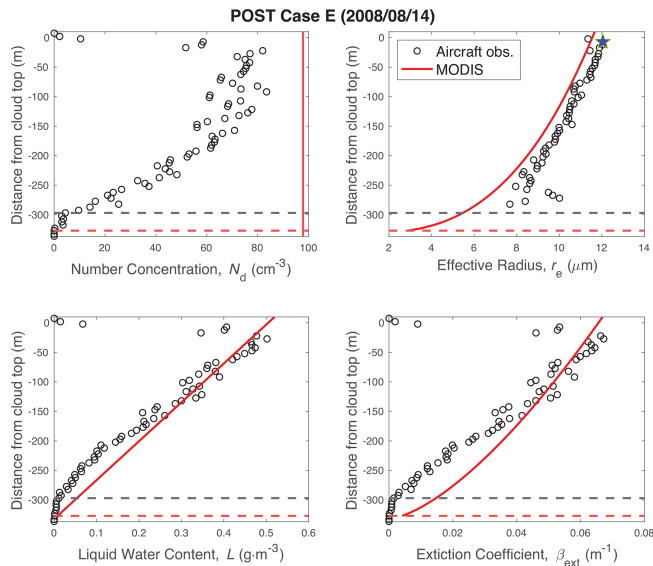


Figure 8. Comparison of profiles of N_d , r_e , L , and β from aircraft observations (circles) and MODIS retrievals (red lines) for POST Case E (14 August 2008). See Fig. 4 for more details.

3.3.5 Case E: POST day 14 August 2008

POST Case E (14 August 2008) illustrates the degree of sensitivity in the MODIS N_d retrieval. Although the agreement between the profiles of r_e , L , and β is not perfect, it is reasonably close (Fig. 8). Despite this, MODIS significantly overestimates the number concentration ($N_d = 98 \pm 5 \text{ cm}^{-3}$ compared to the PDI value of $N_d = 71 \pm 4 \text{ cm}^{-3}$). Even small errors in the effective radius manifest as a large error in the number concentration, presumably due to the non-linear relationship between the two. This result suggests that satellite profile estimates must be fairly accurate in order to successfully retrieve N_d .

3.3.6 Summary of POST cases

Based on POST profile analysis of the important variables that determine the MODIS number concentration, we find that there are cases in which all variables agree well with PDI observations as well as cases where one or more variables disagree. However, out of all eight days considered, there are no cases in which the MODIS N_d was correct due to compensating errors in the underlying variables (i.e., β , L , and r_e). If the satellite number concentration matches the in situ value, it is due to correct estimations in all variables. Conversely, if even one variable disagrees with the observation, N_d is also inaccurate. Fairly good agreement in all three profiles can also still yield a significant discrepancy in N_d .

3.4 Analysis of k and f_{ad}

The accuracy of the MODIS assumptions concerning f_{ad} and k can also affect the retrieved number concentration. The MODIS retrieval assumes that f_{ad} has a constant value of 0.6. If f_{ad} was significantly different from this assumed value, we would find that the assumed MODIS slope of $L(z)$ would disagree with observations. We find that for each of the eight POST flights, the in situ $L(z)$ slopes are well matched to MODIS, even if the absolute values are in disagreement. This leads us to conclude that f_{ad} has little effect on the N_d retrieval for the cases that we analyzed.

The MODIS N_d retrieval assumes k is a constant of value 0.8. The analysis by Grosvenor et al. (2018) concludes that k ranges from 0.7 to 0.9 (see also Lebsock and Witte, 2023). We evaluate this conclusion using the POST data (two examples shown in Fig. 9). Through the bulk of the cloud profiles, the MODIS algorithm assumption is found to be generally reasonable. An uncertainty in k of ± 0.1 will lead to an uncertainty in N_d of 10 % to 15 %. Near the cloud base, k can be much smaller. However, this can be considered inconsequential, as this region contributes little to the MODIS retrievals. There are also cases in which k exceeds this range near the cloud top. However, occasional outlying behavior should not have a large impact on the retrieval and, by default, N_d as well.

3.5 Determination of cloud base

As illustrated by Fig. 5, the large inaccuracies in the MODIS profile assumptions for POST Case B are accompanied by a large satellite overestimation of the cloud base altitude (an over 200 m difference from that observed). Figure 10 compares the MODIS-derived cloud base to the observed cloud base altitude for all eight of the POST flights. MODIS estimates a cloud base height within 50 m of the aircraft observations in five of the eight cases. For the remaining three cases, the MODIS cloud base differs by over 100 m, which is particularly notable because this is a significant fraction of the cloud depth. Due to the small sample size, however, it is difficult to quantify the frequency of accurate MODIS estimations of the cloud base.

4 Conclusions

In this study, we compare N_d derived from MODIS products with in situ observations recorded by the PDI instrument over three different field campaigns (MASE, VOCALS, and POST) sampling marine stratocumulus clouds. We also compare cloud microphysical and radiative variables relevant to the calculation of N_d using observations from the POST campaign. These variables include the vertical profiles of r_e , L , and β .

Our results show that, while there are instances in which the MODIS retrieval predicts a number concentration within

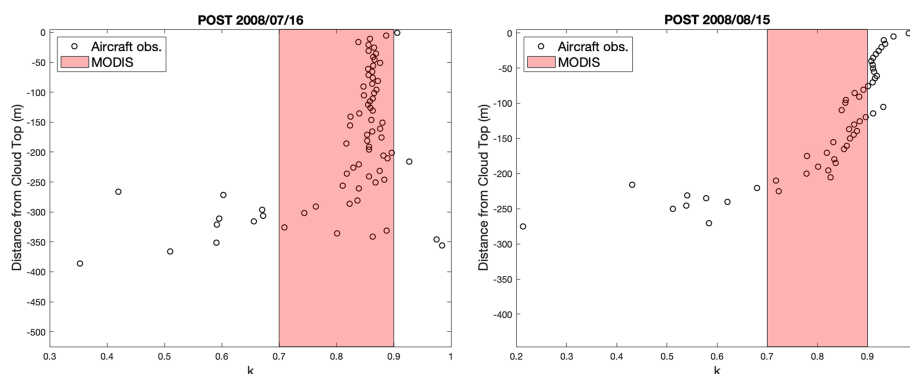


Figure 9. Comparison of k values from the POST campaign for days 16 July 2008 and 15 August 2008 with the MODIS assumed range of $0.7 \leq k \leq 0.9$ (red shading). The PDI values are calculated using Eq. (6) and represent flight averages at each 5 m z_{shift} bin.

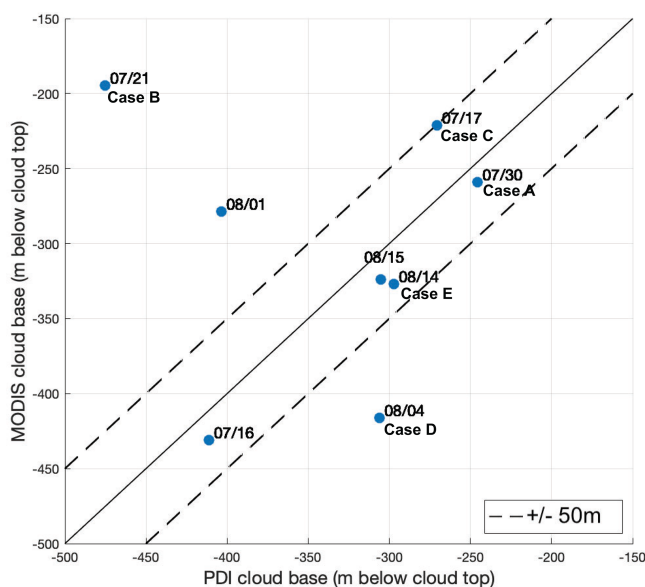


Figure 10. Comparison of the MODIS and aircraft-estimated cloud base altitude for each day of the POST campaign. The 1 : 1 line (solid) and ± 50 m lines (dashed) are also shown.

sampling variability, there are a significant number of cases in which the satellite overestimates N_d . Our results suggest that the discrepancy between retrieved and in situ N_d can be greater than $\pm 50\%$, roughly in line with the $\pm 80\%$ overall uncertainty previously proposed (Bennartz, 2007; Grosvenor et al., 2018). We find that the apparent overestimation bias in the number concentration does not originate as a bias in the MODIS r_e . This finding is consistent with the conclusions of Witte et al. (2018), who found no obvious bias between the MODIS- and PDI-derived effective radius. We also find that it is possible for N_d to be accurately retrieved with a poor retrieval of r_e , presumably due to compensating errors in other retrieval parameters.

Two out of the eight POST cases studied exhibit good agreement in N_d , as well as in the profiles of r_e , L , and β .

For the remaining six cases, we do not attribute N_d discrepancy to a single error source. Instead, we show that there are several different cases that result in an incorrect number concentration:

1. MODIS incorrectly predicts the profiles of r_e , L , and β .
2. MODIS incorrectly predicts the profiles of L and β but accurately estimates r_e (either the full r_e profile or at the most influential altitude near the cloud top).
3. MODIS incorrectly predicts the profiles of r_e but accurately estimates the L and β profiles.

We also show a case where all profiles appear to exhibit reasonably good but imperfect agreement, but the resulting N_d does not agree well at all due to compounding errors.

Accurate N_d retrievals are representative of mid-cloud values. Although MODIS assumes the number concentration is constant through a cloud's vertical profile, it appears to be a poor reflection of cloud top and cloud base conditions even in the best-case scenarios. We also show one case where the assumption that N_d is constant with altitude is not accurate.

In order to improve the MODIS N_d retrieval, it would be beneficial to acquire more data collected in a manner similar to the POST campaign, i.e., with repeated sawtooth-like penetrations through the cloud top. Multiple profiles near the cloud top allow for deeper analysis of the underlying variables in the retrieval, which can be used to more accurately quantify sources of error.

Data availability. The PDI data from POST and VOCALS are freely available at <https://data.eol.ucar.edu/project/96> (UCAR/NCAR – Earth Observing Laboratory, 2024) and <https://data.eol.ucar.edu/project/215> (UCAR/NCAR – Earth Observing Laboratory, 2024), respectively, and those from MASE are available at <https://doi.org/10.5281/zenodo.1035928> (Witte, 2017). Terra MODIS L2 data are available at http://dx.doi.org/10.5067/MODIS/MOD06_L2.061 (Platnick et al., 2015b) and Aqua MODIS L2 data are available at http://dx.doi.org/10.5067/MODIS/MYD06_L2.061 (Platnick et al., 2015a).

Author contributions. SRP performed the data analysis and wrote the manuscript. MKW and PYC designed the study concept, obtained data, and edited the manuscript.

Competing interests. The contact author has declared that none of the authors has any competing interests.

Disclaimer. Publisher's note: Copernicus Publications remains neutral with regard to jurisdictional claims made in the text, published maps, institutional affiliations, or any other geographical representation in this paper. While Copernicus Publications makes every effort to include appropriate place names, the final responsibility lies with the authors.

Acknowledgements. We thank the CIRPAS Twin Otter pilots, crew, and instrument scientists for their efforts to collect the data used in this study.

Financial support. Mikael K. Witte has been supported by the Office of Naval Research Marine Meteorology program under funding documents N0001424WX00817 and N0001424WX02198.

Review statement. This paper was edited by Alexander Kokhanovsky and reviewed by Zachary Lebo and three anonymous referees.

References

- Bellouin, N., Quaas, J., Gryspeerdt, E., Kinne, S., Stier, P., Watson-Parris, D., Boucher, O., Carslaw, K. S., Christensen, M., Daniau, A.-L., Dufresne, J.-L., Feingold, G., Fiedler, S., Forster, P., Gettelman, A., Haywood, J. M., Lohmann, U., Malavelle, F., Mauritsen, T., McCoy, D. T., Myhre, G., Mülmenstädt, J., Neubauer, D., Possner, A., Rugenstein, M., Sato, Y., Schulz, M., Schwartz, S. E., Sourdeval, O., Storelvmo, T., Toll, V., Winker, D., and Stevens, B.: Bounding Global Aerosol Radiative Forcing of Climate Change, *Rev. Geophys.*, 58, e2019RG000660, <https://doi.org/10.1029/2019RG000660>, 2020.
- Bennartz, R.: Global assessment of marine boundary layer cloud droplet number concentration from satellite, *J. Geophys. Res.-Atmos.*, 112, D02201, <https://doi.org/10.1029/2006JD007547>, 2007.
- Bennartz, R. and Rausch, J.: Global and regional estimates of warm cloud droplet number concentration based on 13 years of AQUA-MODIS observations, *Atmos. Chem. Phys.*, 17, 9815–9836, <https://doi.org/10.5194/acp-17-9815-2017>, 2017.
- Carman, J. K., Rossiter, D. L., Khelif, D., Jonsson, H. H., Faloona, I. C., and Chuang, P. Y.: Observational constraints on entrainment and the entrainment interface layer in stratocumulus, *Atmos. Chem. Phys.*, 12, 11135–11152, <https://doi.org/10.5194/acp-12-11135-2012>, 2012.
- Christensen, M. W., Gettelman, A., Cermak, J., Dagan, G., Diamond, M., Douglas, A., Feingold, G., Glassmeier, F., Goren, T., Grosvenor, D. P., Gryspeerdt, E., Kahn, R., Li, Z., Ma, P.-L., Malavelle, F., McCoy, I. L., McCoy, D. T., McFarquhar, G., Mülmenstädt, J., Pal, S., Possner, A., Povey, A., Quaas, J., Rosenfeld, D., Schmidt, A., Schrödner, R., Sorooshian, A., Stier, P., Toll, V., Watson-Parris, D., Wood, R., Yang, M., and Yuan, T.: Opportunistic experiments to constrain aerosol effective radiative forcing, *Atmos. Chem. Phys.*, 22, 641–674, <https://doi.org/10.5194/acp-22-641-2022>, 2022.
- Chuang, P. Y., Saw, E. W., Small, J. D., Shaw, R. A., Sipperley, C. M., Payne, G. A., and Bachalo, W. D.: Airborne phase doppler interferometry for cloud microphysical measurements, *Aerosol Sci. Tech.*, 42, 685–703, <https://doi.org/10.1080/02786820802232956>, 2008.
- Gerber, H., Frick, G., Malinowski, S. P., Jonsson, H., Khelif, D., and Krueger, S. K.: Entrainment rates and microphysics in POST stratocumulus, *J. Geophys. Res.-Atmos.*, 118, 12094–12109, <https://doi.org/10.1002/jgrd.50878>, 2013.
- Gordon, H., Glassmeier, F., and T. McCoy, D.: An Overview of Aerosol-Cloud Interactions, chap. 2, in: *Clouds and Their Climatic Impacts: Radiation, Circulation, and Precipitation*, edited by: Sullivan, S. C. and Hoose, C., American Geophysical Union (AGU), 13–45, <https://doi.org/10.1002/9781119700357.ch2>, 2023.
- Grosvenor, D. P., Sourdeval, O., Zuidema, P., Ackerman, A., Alexandrov, M. D., Bennartz, R., Boers, R., Cairns, B., Chiu, J. C., Christensen, M., Deneke, H., Diamond, M., Feingold, G., Fridlind, A., Hunerbein, A., Knist, C., Kollias, P., Marshak, A., McCoy, D., Merk, D., Painemal, D., Rausch, J., Rosenfeld, D., Russchenberg, H., Seifert, P., Sinclair, K., Stier, P., van Diedenhoven, B., Wendisch, M., Werner, F., Wood, R., Zhang, Z., and Quaas, J.: Remote sensing of droplet number concentration in warm clouds: A review of the current state of knowledge and perspectives, *Rev. Geophys.*, 56, 409–453, <https://doi.org/10.1029/2017RG000593>, 2018.
- Gryspeerdt, E., McCoy, D. T., Crosbie, E., Moore, R. H., Nott, G. J., Painemal, D., Small-Griswold, J., Sorooshian, A., and Ziemba, L.: The impact of sampling strategy on the cloud droplet number concentration estimated from satellite data, *Atmos. Meas. Tech.*, 15, 3875–3892, <https://doi.org/10.5194/amt-15-3875-2022>, 2022.
- Leandro, M. D.: Phase-Doppler Interferometry: Characterization and Emerging Applications, University of California, Santa Cruz, <https://escholarship.org/uc/item/2df8w1zt> (last access: 1 July 2025), 2023.
- Lebsock, M. D. and Witte, M.: Quantifying the dependence of drop spectrum width on cloud drop number concentration for cloud remote sensing, *Atmos. Chem. Phys.*, 23, 14293–14305, <https://doi.org/10.5194/acp-23-14293-2023>, 2023.
- Lu, M.-L., Conant, W. C., Jonsson, H. H., Varutbangkul, V., Flagan, R. C., and Seinfeld, J. H.: The Marine Stratus/Stratocumulus Experiment (MASE): Aerosol-cloud relationships in marine stratocumulus, *J. Geophys. Res.-Atmos.*, 112, D10209, <https://doi.org/10.1029/2006JD007985>, 2007.
- McCoy, D. T., Bender, F. A.-M., Grosvenor, D. P., Mohrmann, J. K., Hartmann, D. L., Wood, R., and Field, P. R.: Predicting decadal trends in cloud droplet number concentration using re-

- analysis and satellite data, *Atmos. Chem. Phys.*, 18, 2035–2047, <https://doi.org/10.5194/acp-18-2035-2018>, 2018.
- McCoy, I. L., McCoy, D. T., Wood, R., Regayre, L., Watson-Parris, D., Grosvenor, D. P., Mulcahy, J. P., Hu, Y., Bender, F. A.-M., Field, P. R., Carslaw, K. S., and Gordon, H.: The hemispheric contrast in cloud microphysical properties constrains aerosol forcing, *P. Natl. Acad. Sci. USA*, 117, 18998–19006, <https://doi.org/10.1073/pnas.1922502117>, 2020.
- Mechoso, C. R., Wood, R., Weller, R., Bretherton, C. S., Clarke, A. D., Coe, H., Fairall, C., Farrar, J. T., Feingold, G., Garreaud, R., Grados, C., McWilliams, J., Szoek, S. P. d., Yuter, S. E., and Zuidema, P.: Ocean Cloud Atmosphere Land Interactions in the Southeastern Pacific: The VOCALS Program, *B. Am. Meteor. Soc.*, 95, 357–375, <https://doi.org/10.1175/BAMS-D-11-00246.1>, 2014.
- Miles, N. L., Verlinde, J., and Clothiaux, E. E.: Cloud droplet size distributions in low-level stratiform clouds, *J. Atmos. Sci.*, 57, 295–311, [https://doi.org/10.1175/1520-0469\(2000\)057<0295:CDSDIL>2.0.CO;2](https://doi.org/10.1175/1520-0469(2000)057<0295:CDSDIL>2.0.CO;2), 2000.
- Min, Q., Joseph, E., Lin, Y., Min, L., Yin, B., Daum, P. H., Kleinman, L. I., Wang, J., and Lee, Y.-N.: Comparison of MODIS cloud microphysical properties with in-situ measurements over the Southeast Pacific, *Atmos. Chem. Phys.*, 12, 11261–11273, <https://doi.org/10.5194/acp-12-11261-2012>, 2012.
- Noble, S. R. and Hudson, J. G.: MODIS comparisons with northeastern Pacific in situ stratocumulus microphysics, *J. Geophys. Res.-Atmos.*, 120, 8332–8344, <https://doi.org/10.1002/2014JD022785>, 2015.
- Painemal, D. and Zuidema, P.: Assessment of MODIS cloud effective radius and optical thickness retrievals over the Southeast Pacific with VOCALS-REx in situ measurements, *J. Geophys. Res.-Atmos.*, 116, D24206, <https://doi.org/10.1029/2011JD016155>, 2011.
- Platnick, S.: Vertical photon transport in cloud remote sensing problems, *J. Geophys. Res.-Atmos.*, 105, 22919–22935, <https://doi.org/10.1029/2000JD900333>, 2000.
- Platnick, S., Ackerman, S., King, M., et al.: MYD06_L2 – MODIS/Aqua Clouds 5-Min L2 Swath 1km and 5km, NASA MODIS Adaptive Processing System [data set], Goddard Space Flight Center, USA, http://dx.doi.org/10.5067/MODIS/MYD06_L2.061, 2015a.
- Platnick, S., Ackerman, S., King, M., et al.: MOD06_L2 – MODIS/Terra Clouds 5-Min L2 Swath 1km and 5km, NASA MODIS Adaptive Processing System [data set], Goddard Space Flight Center, USA, http://dx.doi.org/10.5067/MODIS/MOD06_L2.061, 2015b.
- Quaas, J., Arola, A., Cairns, B., Christensen, M., Deneke, H., Ekman, A. M. L., Feingold, G., Fridlind, A., Gryspeerd, E., Hasekamp, O., Li, Z., Lipponen, A., Ma, P.-L., Mülmenstädt, J., Nenes, A., Penner, J. E., Rosenfeld, D., Schrödner, R., Sinclair, K., Sourdeval, O., Stier, P., Tesche, M., van Diedenhoven, B., and Wendisch, M.: Constraining the Twomey effect from satellite observations: issues and perspectives, *Atmos. Chem. Phys.*, 20, 15079–15099, <https://doi.org/10.5194/acp-20-15079-2020>, 2020.
- Sorooshian, A., Feingold, G., Lebsock, M. D., Jiang, H., and Stephens, G. L.: On the precipitation susceptibility of clouds to aerosol perturbations, *Geophys. Res. Lett.*, 36, L13803, <https://doi.org/10.1029/2009GL038993>, 2009.
- Twomey, S.: The Influence of Pollution on the Shortwave Albedo of Clouds, *J. Atmos. Sci.*, 34, 1149–1152, [https://doi.org/10.1175/1520-0469\(1977\)034<1149:TIOPOT>2.0.CO;2](https://doi.org/10.1175/1520-0469(1977)034<1149:TIOPOT>2.0.CO;2), 1977.
- UCAR/NCAR – Earth Observing Laboratory (EOL): VOCALS: VAMOS Ocean-Cloud-Atmosphere-Land Study, UCAR/NCAR – EOL, <https://data.eol.ucar.edu/project/215> (last access: 2 August 2024), 2024.
- UCAR/NCAR – Earth Observing Laboratory (EOL): POST: Physics of Stratocumulus Top (POST), UCAR/NCAR – EOL [data set], <https://data.eol.ucar.edu/project/96> (last access: 2 August 2024), 2024.
- Witte, M.: MASE cabin and cloud probe data, Version v1, Zenodo [data set], <https://doi.org/10.5281/zenodo.1035928>, 2017.
- Witte, M. K., Yuan, T., Chuang, P. Y., Platnick, S., Meyer, K. G., Wind, G., and Jonsson, H. H.: MODIS retrievals of cloud effective radius in marine stratocumulus exhibit no significant bias, *Geophys. Res. Lett.*, 45, 10,656–10,664, <https://doi.org/10.1029/2018GL079325>, 2018.
- Zheng, X., Albrecht, B., Jonsson, H. H., Khelif, D., Feingold, G., Minnis, P., Ayers, K., Chuang, P., Donaher, S., Rossiter, D., Ghate, V., Ruiz-Plancarte, J., and Sun-Mack, S.: Observations of the boundary layer, cloud, and aerosol variability in the southeast Pacific near-coastal marine stratocumulus during VOCALS-REx, *Atmos. Chem. Phys.*, 11, 9943–9959, <https://doi.org/10.5194/acp-11-9943-2011>, 2011.
- Zhou, X. and Bretherton, C. S.: Simulation of Mesoscale Cellular Convection in Marine Stratocumulus: 2. Nondrizzling Conditions, *J. Adv. Model. Earth Sy.*, 11, 3–18, <https://doi.org/10.1029/2018MS001448>, 2019.